Chapter 11
Nanoarchitectonics Prepared by MAPLE for Biomedical Applications

Roxana Cristina Popescu and Alexandru Mihai Grumezescu

Abstract Thin film depositions by Matrix-Assisted Pulsed Laser Evaporation (MAPLE) technique have been intensively used in order to obtain nanoarchitectonics with different biomedical applications, like drug delivery systems, tissue engineering, implants with improved biocompatibility, improved adherent surfaces, antibacterial surfaces, etc. This chapter presents a description of the latest research regarding magnetite-based thin films and hybrid organic–inorganic thin films obtained by MAPLE. The most encountered preparation methods for magnetite-based thin films and several hybrid organic–inorganic systems are presented. Regarding the biomedical applications, our attention is directed to the antibacterial properties of differently modified surfaces for implants and medical devices.

Keywords Nanoarchitectonics • Thin film deposition • Matrix-assisted pulsed laser evaporation • Magnetite nanoparticles • Hybrid organic–inorganic

11.1 Matrix-Assisted Pulsed Laser Evaporation Technique: General Approach

Thin films are defined as layers of material with a thickness between nanometers to micrometers, while the thin film deposition is a term which refers to the technique of applying a film onto a substrate. The main techniques used for thin film deposition are classified as: (1) laser assisted deposition techniques and (2) non-laser assisted deposition techniques. Laser assisted techniques used for obtaining thin film depositions on different substrates have multiple advantages compared to other

R.C. Popescu • A.M. Grumezescu (✉)
Faculty of Applied Chemistry and Materials Science, Department of Science and Engineering of Oxide Materials and Nanomaterials, University Politehnica of Bucharest, Polizu Street No. 1-7, 011061 Bucharest, Romania
e-mail: grumezescu@yahoo.com

V.A. Basiuk, E.V. Basiuk (eds.), *Green Processes for Nanotechnology*,
DOI 10.1007/978-3-319-15461-9_11

techniques given the following facts: (1) control of the monolayer thickness; (2) strong adhesion of the thin film to the surface of the monolayer; (3) low substrate temperature; (4) ensuring the stoichiometry of precursors; (5) economical consumption of precursors [1]. The main laser-assisted techniques used for the deposition of thin films are: (1) pulsed laser deposition [2, 3]; (2) matrix-assisted pulsed laser evaporation technique [4–6]; (3) spin coating technique [7, 8]; (4) drop casting technique [9].

The interest for laser deposition techniques is given by the fact that the resulted thin films have a controlled topography, which can be manipulated at nanometric level [10]. These materials provide several important applications in the biological field, such as: (1) drug delivery systems [11–13], (2) tissue engineering [14], (3) implants with improved biocompatibility [4, 12], (4) improved adherent surfaces [15, 16], (5) antibacterial surfaces [17, 18], (6) gas sensors [19, 20], etc.

Matrix-assisted pulsed laser evaporation (MAPLE) technique is derived from pulsed laser deposition (PLD) technique, where the target is represented by a frozen homogenous solution of the material of interest, which is diluted in a volatile solvent (matrix solvent). The temperature at which the target solution is frozen is given by the liquid nitrogen temperature. The target is placed in a vacuum chamber and a high energy laser is directed trough it. The pulsed laser energy is absorbed by the solvent in the target and it is converted in thermal energy, which determines the evaporation of the solvent. The evaporating molecules of the solvent collide with the solute (material) molecules, which are transformed in a gas phase, because of the transferred kinetic energy. The advantages of MAPLE compared to PLD are given by the fact that this technique avoids the photochemical damage and the decomposition in PLD technique, which is determined by high energy of the laser pulses [10] (Fig. 11.1).

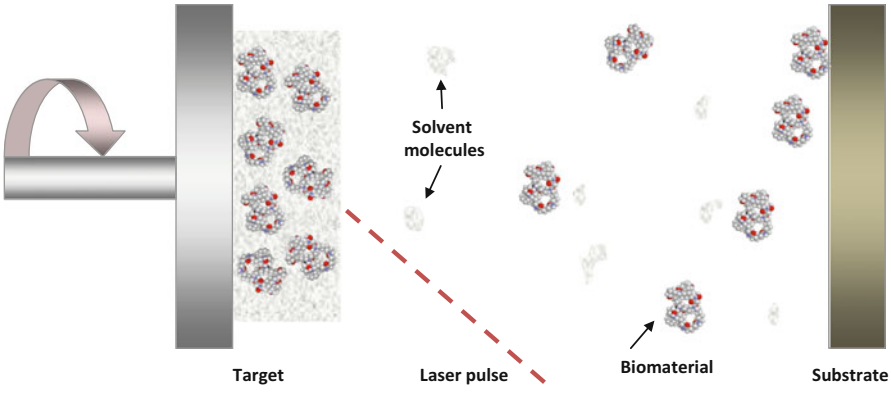

Fig. 11.1 Schematic representation of the principle of matrix-assisted pulsed laser evaporation technique (MAPLE)

11.2 The MAPLE Deposition Apparatus

The MAPLE technique was developed as an improvement for the PLD technique, in order to be used for thin film depositions of organic materials. It was implemented for the first time in the 1990s by the US Naval Research Laboratory to obtain functionalized polymer films [21].

The MAPLE apparatus, as shown in Fig. 11.2, consists of a sealed chamber which presents a cryogenically cooled rotating target holder and a substrate holder, also having a rotation movement. The target holder is connected to a liquid nitrogen tank. The chamber has an input for a background gas and for vacuum. It also presents the laser beam focusing system, which directs pulsating laser beam at a 45° angle, on the target surface [21].

Usually the technique uses an excimer laser such as KrF, with $\lambda = 248$ nm, or ArF, with $\lambda = 193$ nm, and a pulse width between 10 and 30 ns, focused on the target in a 1–10 mm^2 spot. The repetition rate is usually set between 1 and 20 Hz and the laser fluence is between 0.01 and 1.0 J/cm^2, being set according to the type of material (solute) and solvent used to make the target. The process can be held at different pressures, from vacuum, to 70 Pa, in the presence of an inert gas or a background gas [21].

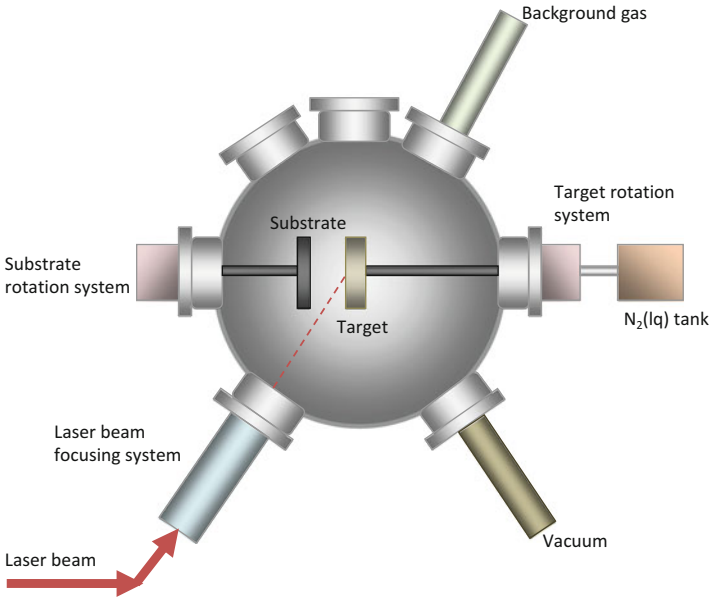

Fig. 11.2 Schematic representation of matrix-assisted pulsed laser evaporation (MAPLE) system; Important parameters in the technological process of MAPLE thin film deposition are the following: (1) the fluency of the laser, (2) the repetition rate, (3) the number of pulses, (4) the target rotation rate, (5) the angle at which the laser beam scans the target surface, (6) the background pressure, (7) the distance between substrate and target [22, 23]

11.3 Thin Films Based on Magnetite Nanostructures

Magnetite nanoparticles are intensively used in different biomedical applications especially due to their magnetic properties [24], biocompatibility [25], and easy obtaining methods [26–28]. Thus, Fe_3O_4 nanoparticle-based materials are used as: (1) drug delivery systems [29–31]; (2) antimicrobial materials [32–34]; (3) hyperthermia applications for cancer treatment [35, 36]; (4) contrast substance for magnetic resonance imaging techniques [35, 37]; etc.

11.3.1 Preparation

Magnetite can be found as a natural mineral, but it can also be artificially obtained using different chemical methods. Fe_3O_4 nanoparticles were obtained for the first time as a ferrofluid in 1981, by Massart [38] using a co-precipitation method, based on the combination of ferric and ferrous salts in an alkaline medium (sodium hydroxide).

Regarding the composition of magnetite, it is an iron oxide consisting of Fe^{3+} and Fe^{2+} ions, with a characteristic molar ratio of Fe^{3+}:Fe^{2+} = 2:1 [39].

The main preparation methods are presented in Table 11.1, where the methods' principle and the implied factors are briefly summarized.

11.3.2 Functionalized Magnetite Nanostructures

The functionalization of nanomaterials consists in modifying the surface of nanoparticles by means of attaching different type of molecules, in order to improve the properties of the inorganic structure: (1) the biocompatibility [50, 51], (2) stability [52, 53], (3) targeting properties [31, 35, 54, 55], (4) carrier properties [56–58] (Fig. 11.3).

Magnetite surface chemistry depends on the pH, acting like Lewis acids in aqueous systems: at low pH values the surface of Fe_3O_4 is positively charged, while at high pH values the magnetite surface is negatively charged [59–61]. The main classes of magnetite functionalization methods are: (1) covalent bonding and (2) non-covalent bonding. The non-covalent bonding between the functionalizing molecules and the magnetite nanoparticle surface is commonly encountered by means of hydrogen bonding with HO^- groups in Fe_3O_4.

The functionalizing agents which can interact with Fe_3O_4 nanoparticles are classified as follows: (1) organic functionalizations and (2) inorganic functionalizations. In the first class are included small molecules and surfactants (dehydroascorbic acid [37], silane compounds [62], folic acid [35], carboxyl [36]) generally applied to reduce the aggregation phenomena of magnetite nanoparticles in suspension;

Table 11.1 The main chemical methods for obtaining Fe_3O_4 nanoparticles

Obtaining method	Method principle	Factors influencing the obtaining process	Observations	References
Co-precipitation	The nucleation process of Fe^{3+} and Fe^{2+} ions takes place in an alkaline medium	Fe^{3+}–Fe^{2+} molar ratio (2:1)	Advantages: high yield synthesis, reproducibility, control of nanoparticle dimensions. Disadvantages: by means of traditional method, aggregation and oxidation of nanoparticles can take place	[26, 39–42]
		pH value (pH = 9-14)		
		Non-oxidant medium		
		Magnetic stirring, ultrasound assisting, mechanical stirring (favors the precursors interaction at molecular level)		
		Using surfactants to control the nanoparticles dimension		
		The crystallization temperature (influences the dimensions of nanoparticles)		
Hydrothermal	Obtaining singular magnetite crystals from water soluble minerals placed in an autoclave; this equipment assures maintaining exact parameters like pressure, temperature and reaction time.	Non-oxidant medium	Advantages: high yield synthesis; controlled technological process; narrow distribution of nanoparticles dimension Disadvantages: long reaction time	[27, 43–47]
		Temperature (influences the dimension of the nanoparticles)		
		Reaction time (influences the dimension of nanoparticles)		
		Pressure (high pressure)		
		Reduction agent (reduces the nanoparticles dimension)		
Solvothermal	Resembles the hydrothermal method, only the precursors are dissolved in organic solvents at a temperature higher that their boiling point.	Time of thermal treatment	Advantages: high control of nanoparticles dimension Disadvantages: The organic solvents used in the obtaining process can be toxic for biological usage	[24, 48, 49]
		Temperature		
		The stabilizer quantity (introduced as organic solvent)		

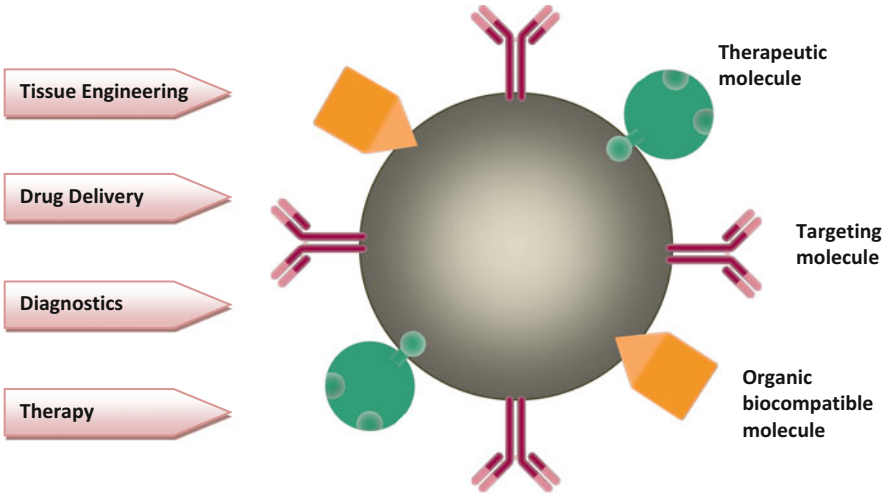

Fig. 11.3 Applications of functionalized magnetite nanoparticles

polymers (PEG [63], chitosan [64], PVA [65]), used to improve biocompatibility, stability, or to modify the character of the nanoparticle surface; enzymes (pullulanase [66], porphyrin [67], glucose oxidase [68]), with sensing properties; respectively, therapeutic molecules (docetaxel [31], usnic acid [32], danorubicin [69], umbelliprenin [70], rotavirus capsid surface protein [57]), used to obtain drug delivery systems. Magnetite functionalization with inorganic coatings is generally applied for different reasons, like: (1) enhancing the magnetic properties of the nanoparticles [71–73]; (2) enhancing the antioxidant properties of magnetite [74]; (3) inducing antibacterial properties [75]; (4) improving the biocompatibility of the system [76, 77].

11.3.3 Thin Films

Magnetite-based thin films can be obtained by several techniques, as follows: (1) pulsed laser deposition technique [78], (2) matrix-assisted laser evaporation technique [79], (3) ultrasound-enhanced ferrite plating [80], (4) chemical vapor deposition [81], (5) DC reactive magnetron sputtering [82] and reactive sputtering [83].

Previously obtained Fe_3O_4 functionalized nanoparticles are prepared as a diluted suspension in the matrix solvent (chloroform 1 % wt./vol.) [84] and then put into a precooled target holder and frozen in liquid nitrogen. For example, Cristescu et al. [84] used the following experimental parameters for all of the Fe_3O_4@oleic acid@ antibiotic MAPLE deposited thin film samples: a laser fluence between 65 and 300 mJ/cm^2, a repetition rate of 10 Hz, 7,200–20,000 laser pulses, a target rotation

rate of 0.4 Hz, an angle of 45° between the laser beam and the target surface, a distance of 4 cm between the substrate and target, and a background pressure of 30–100 Pa [84].

11.3.4 Biological Applications

Nosocomial infections, or hospital-acquired infections, are a current problem of the medical system, over 1.7 million hospital-associated infections contributing and causing over 99.000 deaths every year [85]. In Europe, gram-negative associated infections cause the most numerous untreatable infections [86], therefore combating the antibiotic resistance being an important subject of the latest scientific studies in the biomedical field. Biofilms are microbial communities included in a polysaccharide matrix, attached to a substrate. These are commonly encountered in unsterile prosthetic devices, contributing to a large number of infectious cases. Thus, there are several studies conducted in order to obtain anti-biofilm surface coatings for medical devices, and matrix-assisted pulsed laser evaporation technique offers great solutions; Table 11.2 gives a summary of the latest examples regarding this aspect.

Table 11.2 presents several examples of MAPLE deposited thin films based on modified magnetite nanoparticles, which exhibit antibacterial properties, which can be used as a growth support for cells. The Fe_3O_4@oleic acid/antibiotic thin films are excellent candidates which can be used as surface modification methods for medical devices and implants, with anti-adherence and antimicrobial properties [17]. However, the anti-adherence property refers only to the microbial colonies, as it was proved that human epithelial carcinoma HeLa cell monolayers can grow on these modified surfaces. The antimicrobial properties of the obtained samples were tested against both gram-negative (*Pseudomonas aeruginosa*, *Klebsiella pneumoniae*, *Escherichia coli*) and gram-positive (*Staphylococcus aureus*, *Bacillus subtilis*) bacteria, using the antimicrobial activity assay (API 20E biochemical tests, VITEK I automatic system), to compare the substrate effect with several antibiotic substrates and the microbiological assay investigation procedure to measure the percent of viable bacterial cells attached to the substrates (compared to a control, represented by glass substrate). The in vitro biocompatibility of the obtained samples was evaluated after the addition of the microbial suspensions over the HeLa cell monolayer cultivated on the MAPLE modified substrates. The samples were prepared by Giemsa staining and evaluated using an inverted microscope to conclude over the degree of cell confluency, the cytotoxic effect of nanoparticles, the number of adherent bacteria, and the adherence pattern (localized adherence, where bacteria form microcolonies, diffuse adherence, where bacteria adhere to the whole cell surface and aggregative adherence, where aggregates of bacteria attach to the cells, forming an overlapped arrangement. The cell morphology was not affected by the presence of the nanoparticles, neither was the adherence pattern or the adherence index, compared to control samples.

Table 11.2 Matrix-assisted pulsed laser evaporation technique for anti-biofilm surface coatings

No.	Description	Biological investigations	Reference
1	PLGA–PVA–Fe_3O_4@usnic acid thin film depositions obtained by MAPLE	*Staphylococcus aureus* anti-biofilm adherence surfaces	[87]
2	magnetite/salicylic acid/silica shell/antibiotics thin film depositions obtained by MAPLE	Anti-adherence of *Staphylococcus aureus* and *Pseudomonas aeruginosa* biofilms; biocompatibility proven for eukaryotic HEp-2 cells	[88]
3	Fe_3O_4@oleic acid@ceftriaxone/cefepime thin films deposited by MAPLE onto inert substrates	Microbial viability and microbial adherence tests using gram-negative and gram-positive bacteria proved the antibacterial activity of these films; proved biocompatibility for HeLa cells	[84]
4	Fe_3O_4@*Cinnamomum verum* MAPLE deposited thin films on gastrostomy tubes	Normal development of endothelial cells on the surface of the modified gastrostomy tubes; anti-adherent properties against gram-positive and gram-negative bacteria	[89]
5	PLA–CS–Fe_3O_4@eugenol thin film depositions using MAPLE	The obtained substrates have bioactive properties for human endothelial cells and anti-adherence properties against *Staphylococcus aureus* and *Pseudomonas aeruginosa* bacteria	[90]
6	Poly(3-hydroxybutyric acid-co-3-hydroxyvaleric acid)–polyvinyl alcohol–PVA–Fe_3O_4@eugenol MAPLE deposited thin films	Antibacterial and anti-biofilm characteristics of the obtained thin films proved by viable cell count method on *Staphylococcus aureus* and *Pseudomonas aeruginosa* cultures; biocompatibility proved by analyzing the thin films interaction with EAhy926 human endothelial cells	[79]

Our group obtained Fe_3O_4@eugenol nanoparticles by co-precipitation method, which were embedded in poly(3-hydroxybutyric acid-co-3-hydroxyvaleric acid)–polyvinyl alcohol (P(3HB-3HV)–PVA) microspheres by oil-in-water microemulsion method; these resulted microspheres were used as modifying material for inert substrates [79]. The P(3HB-3HV)–PVA–Fe_3O_4@eugenol thin films were obtained by MAPLE deposition from 1 % (w/v) microsphere suspension in DMSO using a KrF* laser source (248 nm, 25 ns laser pulses, 300–500 mJ/cm^2 laser fluence and a repetition rate of 15 Hz, with 45,000–160,000 laser pulses). The in vitro biocompatibility was evaluated using human endothelial cells EAhy929; the proliferation and viability of the cells was tested using commercial kits, resulting in high viability of

the endothelial cells, the cells' proliferation being increased at 24 h after incubation and being maintained at 48 and 72 h (compared to control). The obtained samples were also tested against biofilm formation for *Staphylococcus aureus* and *Pseudomonas aeruginosa* bacteria using the microbial biofilm assay, which demonstrated the anti-biofilm antibacterial growth effect of the resulted biomaterial.

The same experimental procedure was used by Holban et al. [90] to obtain polylactic acid (PLA)–chitosan (CS)–Fe_3O_4@eugenol microsphere thin films depositions. The in vitro biocompatibility was tested for human endothelial cells EAhy926, using a commercial cell proliferation assay and a fluorescence long term-tracking method. The tests showed that the obtained thin films offer biocompatible support for endothelial cells growth, their morphology and proliferation capability being normal [90]. For the anti-biofilm evaluation, *Staphylococcus aureus* and *Pseudomonas aeruginosa* strains were cultured in Luria Broth medium and put in contact with the resulted biomaterials. The biofilm formation is affected after 24 and 48 h of incubation compared to uncoated magnetite embedded in microspheres control.

Our research group also obtained polylactic-co-glycolic acid (PLGA)–polyvinyl alcohol (PVA)–Fe_3O_4@usnic acid thin film depositions by MAPLE using a KrF* laser source (248 nm, 25 ns laser pulses, 200–400 mJ/cm^2 laser fluence and a repetition rate of 10 Hz, with 10,000–20,000 laser pulses) [87]. The in vitro biocompatibility was evaluated for human mesenchymal stem cells from human bone marrow. The viability of the cultured cells was over 92 %, proving that the obtained thin films can support the normal development of the cells. Also, the normal morphology of the cells showed that the obtained materials have biocompatible properties. To evaluate the antibacterial effect, a minimal inhibitory assay and a microbial adherence and biofilm assay were employed for *S. aureus* bacteria. The obtained thin film inhibited the formation of bacterial strains for 3 days under static conditions, diminishing *S. aureus* adherence and biofilm formation.

Anghel et al. [89] obtained Fe_3O_4@*Cinnamomum verum* MAPLE thin film depositions on gastrostomy tubes, having antibacterial activity against gram-positive (*S. aureus*) and gram-negative (*E. coli*) bacteria [89]. *Cinnamomum verum* is a natural oil with anti-inflammatory, antiseptic, antifungal, and antiviral properties, which can stimulate the immune system and have antioxidant properties. The functionalized magnetite nanoparticles were obtained by co-precipitation method and dispersed in DMSO (1.5 % w/v solution) and frozen in liquid nitrogen. The MAPLE deposition was held using a KrF*laser (248 nm, 25 ns laser pulses, 300–500 mJ/cm^2 laser fluence and a repetition rate of 0.4 Hz, with 30,000–60,000 laser pulses). Regarding the antibacterial effect of the modified tubes, the most inhibitory effect was proved for *S. aureus* (compared to control). The in vitro biocompatibility effect, tested using the MTT assay on human endothelial cells, proved a normal development at 24 and 48 h after incubation, and an improved proliferation at 72 h, compared to control. The fluorescence microscopy images obtained at 5 days after incubation showed a normal growth and morphology of the cells.

11.4 Thin Films Based on Inorganic–Organic Hybrid Nanomaterials

Hybrid organic–inorganic nanomaterials have been intensively used in different biomedical applications due to the combination of properties from both organic and inorganic moieties [91]. Examples of such applications are: (1) tissue engineering [15], (2) antibacterial and anti-biofilm effect [92], (3) drug delivery systems [93].

There are several reasons for developing such materials, excelling in the improvement of properties like: (1) increased biocompatibility of the designed nanomaterials, by applying several organic functionalizing agents; (2) antibacterial properties of the organic material; (3) increased stability; (4) modifying the surface character; (5) drug loading.

11.4.1 Preparation

The preparation of hybrid nanomaterials can be done in several ways, which are grouped in two main classes, depending on the interactions that take place between the organic and inorganic phases: (1) methods where no covalent bond is formed between the two phases, (2) methods where covalent bonds are formed between the two phases. Table 11.3 [94] summarizes the main methods for obtaining organic–inorganic hybrid nanomaterials (Fig. 11.4).

11.4.2 Thin Films

Birjega et al. [119] obtained layered double hydroxide (LDH)–polyethylene glycol (PEG)/ethylene glycol (EG) thin films deposited by MAPLE technique [119]. The interest for LDH is given by the fact that it is an artificial clay, which consists of positively charged layers, arranged parallel one to another. It acts as a host material for anions located in the interlayer regions, which can be easily replaced by other negatively charged molecules of biological interest. The main application of these thin film coatings consists in modifying the surface character and controls its surface wetting. The Mg-Al LDH (Mg/Al = 3) was obtained using a co-precipitation method (at suprasaturation, pH = 10) from aqueous solutions of Mg and Al nitrates, sodium hydroxide and carbonate, resulting in a gel, which underwent a drying process (85 °C, 24 h), followed by a calcination process (460 °C, 18 h, nitrogen atmosphere). LDH-polymer (PEG/EG) composites were prepared by immersing Mg(Al)O mixed oxides powders immersed in aqueous polymer solutions (200 amu/1,450 amu, where Mg(Al)O/PEG and Mg(Al)O/EG = 1.76/1), separated by vacuum filtration and dried (vacuum, 30 °C, 24 h) [119]. For MAPLE deposition of the thin films, a Nd:YAG laser (266 nm, 5 ns pulses, with a repetition rate of 10Hz, a laser fluence of 1–2 J/cm^2) was used. Other important parameters are: (1) a

Table 11.3 Methods for obtaining organic–inorganic nanomaterials [94]

Class of methods	Method	Method description	Examples	Reference
Non covalent bond	Addition of pre-obtained nanoparticles in polymer solutions	Disadvantages: homogeneity of the resulted material; possible aggregation of nanoparticles	Psyllium-aspirin-TiO_2 for controlled delivery	[95]
			Bio-based phase change materials (fatty acids)-exfoliated graphite nanoplatelets/carbon nanotubes	[96]
			Polyacrylic acid- TiO_2	[97]
	In situ formation of nanoparticles		Polyamide-SiO_2	[98]
			Melamine- Ag	[99]
			Poly (vinylidene fluoride)- Ag	[100]
	Monomer polymerization in the inorganic material pores	Disadvantages: the polymerization process needs an initiator which can be toxic (usually this method has a phase of radical polymerization)	Poly L-lactide- layered double hydroxide	[101]
			Polyacrylamide-layered double hydroxide	[102]
			poly(methyl methacrylate)-layered double hydroxide	[103]
	Small molecules encapsulation	Advantages: this is a common method used to obtain drug delivery systems	$CaCO_3$–Lysozyme	[104]
			SiO_2–hemoglobin	[105]
			$CaCO_3$–Vaterite	[106]
	Interpenetrating networks	Advantages: both organic and inorganic parts grow simultaneously Disadvantages: the growing process of both phases must take place at similar rates; the process has little reproducibility	ZrO_2/PEG	[107]
			Polypropylene-silica	[108]
	Self-assembly	Advantages: High strength and stability	Gelatin-CaP	[109]

(continued)

Table 11.3 (continued)

Class of methods	Method	Method description	Examples		Reference
Covalent bond	Covalent linking at molecular level	Advantages: Improved dispersion of the modified nanoparticles	Surface polymerization	Poly(methyl methacrylate)- carbon doped TiO_2	[110]
				Poly(methyl methacrylate-(3-mercaptopropyl) trimethoxysilane–Fe_3O_4	[111]
				Poly(hydroethyl acrylate–bromo-acetamide–ZnO	[112]
	Covalent linking between a pre-obtained polymer and an inorganic nanoparticle	The method can be applied easily for polymers having a carboxyl group which can react with metal oxide nanoparticles	3-aminopropyltrimethoxysilane/3-Isocyanatopropyl trimethoxysilane- TiO_2 (condensation reaction)		[113]
			Poly(vinyl alcohol)–γ-aminopropyltriethoxy silane–TiO_2		[114]
			Amino propyl trimethoxy silane- TiO_2 (condensation reaction)		[115]
	Templating	Advantages: high precision and reproducible properties	Polyvinylidene fluoride- TiO_2- 1H,1H,2H,2H-perfluorododecyltrichlorosilane		[116]
			TiO_2–polyethylene glycol–SiO_2		[117]
			TiO_2–palygorskite		[118]

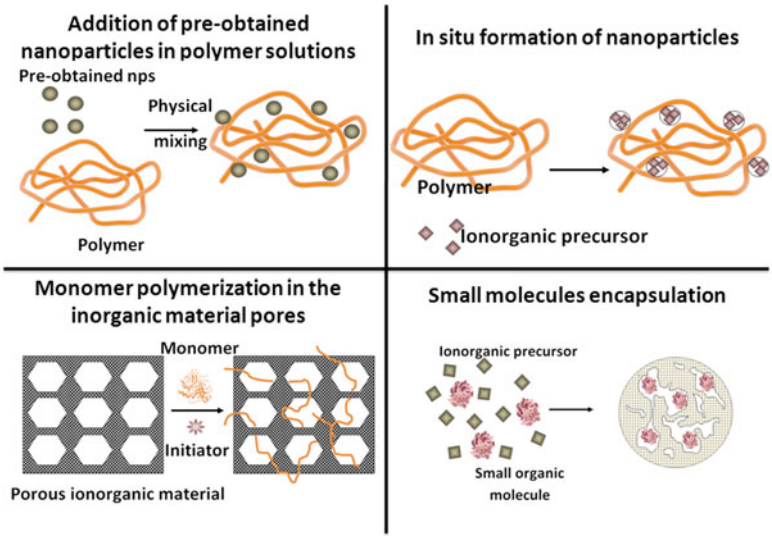

Fig. 11.4 Schematic representations of non-covalent bonding methods for obtaining hybrid nanomaterials

45° angle between the laser and the target; (2) a laser spot size between 0.6 and 0.8 mm^2; (3) 40,000–60,000 laser pulses.

Predoi et al. obtained γ-Fe_2O_3@dextran thin films deposited by MAPLE technique using a UV KrF* excimer laser (248 nm), with 25 ns pulses and a repetition rate of 10 Hz. 25×10^3 laser pulses were applied and a fluence of 0.5 J/cm^2 was assured [120]. The target was prepared using a solution of 0–25 wt.% iron oxide nanoparticles obtained by co-precipitation method, 10 wt.% dextran (2,500 Da) and distillated, frozen in liquid nitrogen solution. The surface morphology of the obtained samples was investigated by scanning electron microscopy technique, which proved an aggregated aspect of the films, consisting of micrometer sized grains. Also, by other investigations, the authors concluded that the resulted thin films have a crystallinity, chemical composition, and molecular structure identical to the materials used for target preparation.

In the experiment described by Miroiu et al. [15], hydroxyapatite–silk fibroin thin films were obtained by MAPLE deposition. The target was prepared using polymer solutions (2 wt.% and 4 wt.%, respectively) and adding hydroxyapatite (HA) in order to obtain a HA–fibroin weight ratio of about 3:2 and 3:4 respectively. The HA–fibroin solutions were mechanically stirred and several drops of NaOH or NaCl were added in order to adjust the pH to 7.4 (physiological value). Then, the solutions were frozen in liquid nitrogen to obtain the targets. For the deposition process, a KrF* excimer laser (248 nm, with 25 ns pulses, a repetition rate of 10–15 Hz and a laser fluence of 0.4–0.5 J/cm^2) was used; 20,000–50,000 pulses were applied for each film [15].

11.4.3 Biological Applications

Miroiu et al. obtained hydroxyapatite–silk fibroin thin films deposited by MAPLE on the surface of metallic prosthesis. The aim of the study was given by the fact that the biomimetic modifies surface display enhanced properties like bioaffinity and osteoconductivity. The in vitro biocompatibility test using SaOs2 osteosarcoma cells cultured for 72 h on the surface of the modified implants showed an improved viability and spreading of the cells. The elongated morphology of the cells proved that the resulted hydroxyapatite–silk fibroin coatings have good performances as bone implants, assuring an optimal interface between the living tissue and the metallic surface of the prosthesis. The best results were given by the HA3-FIB4 sample (3 wt% hydroxyapatite–4 wt% fibroin) [15].

The γ-Fe_2O_3@dextran thin film depositions obtained using MAPLE technique by Predoi et al. [120] were investigated as biocompatible structures used for implant modification coatings in locoregional cancer treatment by hyperthermia after a surgical intervention. Thus, human hepatocarcinoma cells HepG2 were cultivated on the obtained thin films, the viability investigated by MTT colorimetric assay, resulting in a good biocompatibility of the materials. Regarding the morphological aspect of the cells, the cells cultured on the 5 wt.% iron oxide samples grew into larger multicellular aggregates [120] (Table 11.4).

11.5 Conclusions and Perspectives

Matrix-assisted pulsed laser evaporation is the most frequently used method to obtain thin film nanoarchitectonics for biomedical applications, because of its numerous advantages, like assuring control of the monolayer thickness, a strong adhesion of the thin film to the surface of the monolayer, low substrate temperature, ensuring the stoichiometry of precursors, and economical consumption of precursors. This technique has been applied to obtain magnetite modified surfaces with antibacterial properties, used for implants and medical devices, in order to prevent the nosocomial infections, frequently associated with improper sterilization or surgical procedures. However, these systems do not affect the adherence and biocompatibility of tissue cells. Hybrid organic–inorganic nanomaterials are preferred because they combine properties from both components, resulting in an increased biocompatibility of the designed nanomaterials, by applying several organic functionalizing agents, antibacterial properties of the organic material, increased stability, a modified surface character, drug loading. Such thin films have been applied for modified surface prosthesis with antibacterial properties and improved biocompatibility and cellular adherence. Some systems have been designed for delivery action, in order to improve some properties, or for therapeutic effects.

Table 11.4 Classes of organic–inorganic thin film depositions using MAPLE

Class of inorganic material	Description of the system	Biological application	Biological evaluation	Reference
Silver-based	PEG–PLGA–AgNPs thin film depositions by MAPLE	Antibacterial properties	In vitro antibacterial activity against *Escherichia coli*	[121]
Calcium-based	Alendronate–hydroxyapatite deposited thin films by MAPLE	Tissue engineering (enhanced bioactivity)	In vitro interaction with osteoblast-like MG-63 cells and human osteoclasts; normal morphology, increased proliferation, high differentiation parameters for osteoblast cells; reduced proliferation of osteoclasts	[122]
	Hydroxyapatite@ maleate-vinyl acetate thin film deposition by MAPLE	Bone implantology	In vitro biocompatibility evaluation using human primary osteoblasts (OBs); specific and controlled proliferation (indicated by the measurements of collagen and non-collagenous proteins); normal cytoskeleton and vinculin dynamics indicating the adherence of OBs at the substrate	[123]
Silica-based	Fe_3O_4@salicylic acid@ SiO_2@ antibiotic MAPLE thin films	Antibacterial properties	In vitro biocompatibility evaluation using HEp-2 cells; in vitro anti-biofilm evaluation against *Staphylococcus aureus* and *Pseudomonas aeruginosa* strains	[88]
Iron oxide-based	γ-Fe_2O_3@dextran thin films obtained by MAPLE depositions	Biocompatible substrates	In vitro biocompatibility evaluation using Hep G2 cells (human liver cells); fluorescence visualization proved a normal development of actin cytoskeleton and a normal cell cycle	[124]

Acknowledgements This work was financially supported by Sectoral Operational Programme Human Resources Development, financed from the European Social Fund and by the Romanian Government under the contract number POSDRU/156/1.2/G/135764 "Improvement and implementation of university master programs in the field of Applied Chemistry and Materials Science–ChimMaster".

References

1. Wu PK, Ringeisen BR, Callahan J, Brooks M, Bubb DM, Wu HD, Pique A, Spargo B, McGill RA, Chrisey DB (2001) The deposition, structure, pattern deposition, and activity of biomaterial thin-films by matrix-assisted pulsed-laser evaporation (MAPLE) and MAPLE direct write. Thin Solid Films 398:607–614
2. Erakovic S, Jankovic A, Ristoscu C, Duta L, Serban N, Visan A, Mihailescu IN, Stan GE, Socol M, Iordache O, Dumitrescu I, Luculescu CR, Janackovic D, Miskovic-Stankovic V (2014) Antifungal activity of Ag:hydroxyapatite thin films synthesized by pulsed laser deposition on Ti and Ti modified by TiO_2 nanotubes substrates. Appl Surf Sci 293:37–45
3. Duta L, Oktar FN, Stan GE, Popescu-Pelin G, Serban N, Luculescu C, Mihailescu IN (2013) Novel doped hydroxyapatite thin films obtained by pulsed laser deposition. Appl Surf Sci 265:41–49
4. Visan A, Grossin D, Stefan N, Duta L, Miroiu FM, Stan GE, Sopronyi M, Luculescu C, Freche M, Marsan O, Charvilat C, Ciuca S, Mihailescu IN (2014) Biomimetic nanocrystalline apatite coatings synthesized by Matrix Assisted Pulsed Laser Evaporation for medical applications. Mater Sci Eng B-Adv 181:56–63
5. Iordache S, Cristescu R, Popescu AC, Popescu CE, Dorcioman G, Mihailescu IN, Ciucu AA, Balan A, Stamatin I, Fagadar-Cosma E, Chrisey DB (2013) Functionalized porphyrin conjugate thin films deposited by matrix assisted pulsed laser evaporation. Appl Surf Sci 278:207–210
6. Palla-Papavlu A, Rusen L, Dinca V, Filipescu M, Lippert T, Dinescu M (2014) Characterization of ethylcellulose and hydroxypropyl methylcellulose thin films deposited by matrix-assisted pulsed laser evaporation. Appl Surf Sci 302:87–91
7. Heredia E, Bojorge C, Casanova J, Cánepa H, Craievich A, Kellermann G (2014) Nanostructured ZnO thin films prepared by sol–gel spin-coating. Appl Surf Sci 317:19–25, http://dx.doi.org/10.1016/j.apsusc.2014.08.046
8. Carradò A, Viart N (2010) Nanocrystalline spin coated sol–gel hydroxyapatite thin films on Ti substrate: Towards potential applications for implants. Solid State Sci 12(7):1047–1050, http://dx.doi.org/10.1016/j.solidstatesciences.2010.04.014
9. Farag AAM, Yahia IS (2010) Structural, absorption and optical dispersion characteristics of rhodamine B thin films prepared by drop casting technique. Opt Commun 283(21): 4310–4317
10. Caricato AP, Luches A, Leggieri G, Martino M, Rella R (2012) Matrix-assisted pulsed laser deposition of polymer and nanoparticle films. Vacuum 86(6):661–666
11. Paun IA, Moldovan A, Luculescu CR, Dinescu M (2011) Biocompatible polymeric implants for controlled drug delivery produced by MAPLE. Appl Surf Sci 257(24):10780–10788
12. Sima F, Axente E, Iordache I, Luculescu C, Gallet O, Anselme K, Mihailescu N (2014) Combinatorial matrix assisted pulsed laser evaporation of a biodegradable polymer and fibronectin for protein immobilization and controlled release. Appl Surf Sci 306:75–79
13. Paun IA, Moldovan A, Luculescu CR, Staicu A, Dinescu M (2012) MAPLE deposition of PLGA:PEG films for controlled drug delivery: Influence of PEG molecular weight. Appl Surf Sci 258(23):9302–9308
14. Mihailescu M, Popescu RC, Matei A, Acasandrei A, Paun IA, Dinescu M (2014) Investigation of osteoblast cells behavior in polymeric 3D micropatterned scaffolds using digital holographic microscopy. Appl Optics 53(22):4850–4858

15. Miroiu FM, Socol G, Visan A, Stefan N, Craciun D, Craciun V, Dorcioman G, Mihailescu IN, Sima LE, Petrescu SM, Andronie A, Stamatin I, Moga S, Ducu C (2010) Composite biocompatible hydroxyapatite–silk fibroin coatings for medical implants obtained by Matrix Assisted Pulsed Laser Evaporation. Mater Sci Eng B 169(1–3):151–158, http://dx.doi.org/10.1016/j.mseb.2009.10.004
16. Rusen L, Dinca V, Mitu B, Mustaciosu C, Dinescu M (2014) Temperature responsive functional polymeric thin films obtained by matrix assisted pulsed laser evaporation for cells attachment–detachment study. Appl Surf Sci 302:134–140, http://dx.doi.org/10.1016/j.apsusc.2013.09.122
17. Cristescu R, Popescu C, Dorcioman G, Miroiu FM, Socol G, Mihailescu IN, Gittard SD, Miller PR, Narayan RJ, Enculescu M, Chrisey DB (2013) Antimicrobial activity of biopolymer–antibiotic thin films fabricated by advanced pulsed laser methods. Appl Surf Sci 278:211–213, http://dx.doi.org/10.1016/j.apsusc.2013.01.062
18. Grumezescu V, Socol G, Grumezescu AM, Holban AM, Ficai A, Truşcă R, Bleotu C, Balaure PC, Cristescu R, Chifiriuc MC (2014) Functionalized antibiofilm thin coatings based on PLA–PVA microspheres loaded with usnic acid natural compounds fabricated by MAPLE. Appl Surf Sci 302:262–267, http://dx.doi.org/10.1016/j.apsusc.2013.09.081
19. Caricato AP, Luches A, Rella R (2009) Nanoparticle thin films for Gas sensors prepared by matrix assisted pulsed laser evaporation. Sensors (Basel) 9(4):2682–2696
20. Kopecky D, Vrnata M, Vyslouzil F, Myslik V, Fitl P, Ekrt O, Matejka P, Jelinek M, Kocourek T (2009) Polypyrrole thin films for gas sensors prepared by matrix-assisted pulsed laser evaporation technology: effect of deposition parameters on material properties. Thin Solid Films 517(6):2083–2087
21. Pique A (2011) The matrix-assisted pulsed laser evaporation (MAPLE) process: origins and future directions. Appl Phys A-Mater 105(3):517–528
22. Itina TE, Zhigilei LV, Garrison BJ (2001) Matrix-assisted pulsed laser evaporation of polymeric materials: a molecular dynamics study. Nucl Instrum Meth B 180:238–244
23. Bubb DM, Papantonakis M, Collins B, Brookes E, Wood J, Gurudas U (2007) The influence of solvent parameters upon the surface roughness of matrix assisted laser deposited thin polymer films. Chem Phys Lett 448(4–6):194–197
24. Jia K, Zhang J, Huang X, Liu X (2014) Size dependent electromagnetic properties of Fe_3O_4 nanospheres. Chem Phys Lett 614:31–35, http://dx.doi.org/10.1016/j.cplett.2014.09.002
25. Xiao L, Li J, Brougham DF, Fox EK, Feliu N, Bushmelev A, Schmidt A, Mertens N, Kiessling F, Valldor M, Fadeel B, Mathur S (2011) Water-soluble superparamagnetic magnetite nanoparticles with biocompatible coating for enhanced magnetic resonance imaging. ACS Nano 5(8):6315–6324
26. Anbarasu M, Anandan M, Chinnasamy E, Gopinath V, Balamurugan K (2015) Synthesis and characterization of polyethylene glycol (PEG) coated Fe_3O_4 nanoparticles by chemical co-precipitation method for biomedical applications. Spectrochim Acta A Mol Biomol Spectrosc 135:536–539, http://dx.doi.org/10.1016/j.saa.2014.07.059
27. Ahmadi S, Chia CH, Zakaria S, Saeedfar K, Asim N (2012) Synthesis of Fe_3O_4 nanocrystals using hydrothermal approach. J Magn Magn Mater 324(24):4147–4150
28. Li YF, Jiang RL, Liu TY, Lv H, Zhou L, Zhang XY (2014) One-pot synthesis of grass-like Fe_3O_4 nanostructures by a novel microemulsion-assisted solvothermal method. Ceram Int 40(1):1059–1063
29. Gu L, He XM, Wu ZY (2014) Mesoporous Fe_3O_4/hydroxyapatite composite for targeted drug delivery. Mater Res Bull 59:65–68
30. Yan SF, Zhang X, Sun YY, Wang TT, Chen XS, Yin JB (2014) In situ preparation of magnetic Fe_3O_4 nanoparticles inside nanoporous poly(L-glutamic acid)/chitosan microcapsules for drug delivery. Colloid Surf B 113:302–311
31. Huang X, Yi C, Fan Y, Zhang Y, Zhao L, Liang Z, Pan J (2014) Magnetic Fe3O4 nanoparticles grafted with single-chain antibody (scFv) and docetaxel loaded β-cyclodextrin potential for ovarian cancer dual-targeting therapy. Mater Sci Eng C 42:325–332, http://dx.doi.org/10.1016/j.msec.2014.05.041

32. Grumezescu AM, Holban AM, Andronescu E, Mogosanu GD, Vasile BS, Chifiriuc MC, Lazar V, Andrei E, Constantinescu A, Maniu H (2014) Anionic polymers and 10 nm Fe_3O_4@ UA wound dressings support human foetal stem cells normal development and exhibit great antimicrobial properties. Int J Pharm 463(2):146–154
33. Amarjargal A, Tijing LD, Im I-T, Kim CS (2013) Simultaneous preparation of Ag/Fe_3O_4 core–shell nanocomposites with enhanced magnetic moment and strong antibacterial and catalytic properties. Chem Eng J 226:243–254, http://dx.doi.org/10.1016/j.cej.2013.04.054
34. Fang WJ, Zheng J, Chen C, Zhang HB, Lu YX, Ma L, Chen GJ (2014) One-pot synthesis of porous Fe_3O_4 shell/silver core nanocomposites used as recyclable magnetic antibacterial agents. J Magn Magn Mater 357:1–6
35. Jiang QL, Zheng SW, Hong RY, Deng SM, Guo L, Hu RL, Gao B, Huang M, Cheng LF, Liu GH, Wang YQ (2014) Folic acid-conjugated Fe_3O_4 magnetic nanoparticles for hyperthermia and MRI in vitro and in vivo. Appl Surf Sci 307:224–233
36. Barick KC, Singh S, Bahadur D, Lawande MA, Patkar DP, Hassan PA (2014) Carboxyl decorated Fe_3O_4 nanoparticles for MRI diagnosis and localized hyperthermia. J Colloid Interface Sci 418:120–125
37. Gupta H, Paul P, Kumar N, Baxi S, Das DP (2014) One pot synthesis of water-dispersible dehydroascorbic acid coated Fe_3O_4 nanoparticles under atmospheric air: Blood cell compatibility and enhanced magnetic resonance imaging. J Colloid Interface Sci 430:221–228, http://dx.doi.org/10.1016/j.jcis.2014.05.043
38. Massart R (1981) Preparation of aqueous magnetic liquids in alkaline and acidic media. IEEE T Magn 17(2):1247–1248
39. Faiyas APA, Vinod EM, Joseph J, Ganesan R, Pandey RK (2010) Dependence of pH and surfactant effect in the synthesis of magnetite (Fe_3O_4) nanoparticles and its properties. J Magn Magn Mater 322(4):400–404
40. Lin CC, Ho JM (2014) Structural analysis and catalytic activity of Fe_3O_4 nanoparticles prepared by a facile co-precipitation method in a rotating packed bed. Ceram Int 40(7): 10275–10282
41. Maier-Hauff K, Ulrich F, Nestler D, Niehoff H, Wust P, Thiesen B, Orawa H, Budach V, Jordan A (2011) Efficacy and safety of intratumoral thermotherapy using magnetic iron-oxide nanoparticles combined with external beam radiotherapy on patients with recurrent glioblastoma multiforme. J Neuro-Oncol 103(2):317–324
42. Meng HN, Zhang ZZ, Zhao FX, Qiu T, Yang JD (2013) Orthogonal optimization design for preparation of Fe_3O_4 nanoparticles via chemical coprecipitation. Appl Surf Sci 280:679–685
43. Ma FX, Sun XY, He K, Jiang JT, Zhen L, Xu CY (2014) Hydrothermal synthesis, magnetic and electromagnetic properties of hexagonal Fe_3O_4 microplates. J Magn Magn Mater 361:161–165
44. Yang XW, Jiang W, Liu L, Chen BH, Wu SX, Sun DP, Li FS (2012) One-step hydrothermal synthesis of highly water-soluble secondary structural Fe_3O_4 nanoparticles. J Magn Magn Mater 324(14):2249–2257
45. Yuan KF, Ni YH, Zhang L (2012) Facile hydrothermal synthesis of polyhedral Fe_3O_4 nanocrystals, influencing factors and application in the electrochemical detection of H_2O_2. J Alloy Compd 532:10–15
46. Wu R, Liu J-H, Zhao L, Zhang X, Xie J, Yu B, Ma X, Yang S-T, Wang H, Liu Y (2014) Hydrothermal preparation of magnetic Fe3O4@C nanoparticles for dye adsorption. J Environ Chem Eng 2(2):907–913, http://dx.doi.org/10.1016/j.jece.2014.02.005
47. Gao G, Qiu PY, Qian QR, Zhou N, Wang K, Song H, Fu HL, Cui DX (2013) PEG-200-assisted hydrothermal method for the controlled-synthesis of highly dispersed hollow Fe_3O_4 nanoparticles. J Alloy Compd 574:340–344
48. Chen FX, Liu R, Xiao SW, Zhang CT (2014) Solvothermal synthesis in ethylene glycol and adsorption property of magnetic Fe_3O_4 microspheres. Mater Res Bull 55:38–42
49. Liu J, Wang L, Wang J, Zhang LT (2013) Simple solvothermal synthesis of hydrophobic magnetic monodispersed Fe_3O_4 nanoparticles. Mater Res Bull 48(2):416–421

50. Patil RM, Shete PB, Thorat ND, Otari SV, Barick KC, Prasad A, Ningthoujam RS, Tiwale BM, Pawar SH (2014) Superparamagnetic iron oxide/chitosan core/shells for hyperthermia application: Improved colloidal stability and biocompatibility. J Magn Magn Mater 355:22–30
51. Wei Y, Yin GF, Ma CY, Huang ZB, Chen XC, Liao XM, Yao YD, Yin H (2013) Synthesis and cellular compatibility of biomineralized Fe_3O_4 nanoparticles in tumor cells targeting peptides. Colloid Surf B 107:180–188
52. Nigam S, Barick KC, Bahadur D (2011) Development of citrate-stabilized Fe_3O_4 nanoparticles: conjugation and release of doxorubicin for therapeutic applications. J Magn Magn Mater 323(2):237–243
53. Safari J, Masouleh SF, Zarnegar Z, Najafabadi AE (2014) Water-dispersible Fe_3O_4 nanoparticles stabilized with a biodegradable amphiphilic copolymer. C R Chim 17(2):151–155
54. Sohn C-H, Park SP, Choi SH, Park S-H, Kim S, Xu L, Kim S-H, Hur JA, Choi J, Choi TH (2015) MRI molecular imaging using GLUT1 antibody-Fe_3O_4 nanoparticles in the hemangioma animal model for differentiating infantile hemangioma from vascular malformation. Nanomedicine 11(1):127–135, http://dx.doi.org/10.1016/j.nano.2014.08.003
55. Tran LD, Hoang NMT, Mai TT, Tran HV, Nguyen NT, Tran TD, Do MH, Nguyen QT, Pham DG, Ha TP, Le HV, Nguyen PX (2010) Nanosized magnetofluorescent Fe_3O_4–curcumin conjugate for multimodal monitoring and drug targeting. Colloids Surf A Physicochem Eng Asp 371(1–3):104–112, http://dx.doi.org/10.1016/j.colsurfa.2010.09.011
56. Chen CY, Jiang XC, Kaneti YV, Yu AB (2013) Design and construction of polymerized-glucose coated Fe3O4 magnetic nanoparticles for delivery of aspirin. Powder Technol 236:157–163
57. Chen WH, Cao YH, Liu M, Zhao QH, Huang J, Zhang HL, Deng ZW, Dai JW, Williams DF, Zhang ZJ (2012) Rotavirus capsid surface protein VP4-coated Fe_3O_4 nanoparticles as a theranostic platform for cellular imaging and drug delivery. Biomaterials 33(31):7895–7902
58. Lu WS, Shen YH, Xie AJ, Zhang WQ (2013) Preparation and drug-loading properties of Fe_3O_4/Poly(styrene-co-acrylic acid) magnetic polymer nanocomposites. J Magn Magn Mater 345:142–146
59. Hajdu A, Illes E, Tombacz E, Borbath I (2009) Surface charging, polyanionic coating and colloid stability of magnetite nanoparticles. Colloid Surf A 347(1–3):104–108
60. Tombacz E, Toth IY, Nesztor D, Illes E, Hajdu A, Szekeres M, Vekas L (2013) Adsorption of organic acids on magnetite nanoparticles, pH-dependent colloidal stability and salt tolerance. Colloid Surf A 435:91–96
61. Salazar-Camacho C, Villalobos M, Rivas-Sanchez MD, Arenas-Alatorre J, Alcaraz-Cienfuegos J, Gutierrez-Ruiz ME (2013) Characterization and surface reactivity of natural and synthetic magnetites. Chem Geol 347:233–245
62. Atila Dinçer C, Yıldız N, Aydoğan N, Çalımlı A (2014) A comparative study of Fe_3O_4 nanoparticles modified with different silane compounds. Appl Surf Sci 318:297–304, http://dx.doi.org/10.1016/j.apsusc.2014.06.069
63. Yang JH, Zou P, Yang LL, Cao J, Sun YF, Han DL, Yang S, Wang Z, Chen G, Wang BJ, Kong XW (2014) A comprehensive study on the synthesis and paramagnetic properties of PEG-coated Fe_3O_4 nanoparticles. Appl Surf Sci 303:425–432
64. Shariatinia Z, Nikfar Z (2013) Synthesis and antibacterial activities of novel nanocomposite films of chitosan/phosphoramide/Fe_3O_4 NPs. Int J Biol Macromol 60:226–234
65. Ghanbari D, Salavati-Niasari M, Ghasemi-Kooch M (2014) A sonochemical method for synthesis of Fe_3O_4 nanoparticles and thermal stable PVA-based magnetic nanocomposite. J Ind Eng Chem 20(6):3970–3974, http://dx.doi.org/10.1016/j.jiec.2013.12.098
66. Long J, Jiao A, Wei B, Wu Z, Zhang Y, Xu X, Jin Z (2014) A novel method for pullulanase immobilized onto magnetic chitosan/Fe_3O_4 composite nanoparticles by in situ preparation and evaluation of the enzyme stability. J Mol Catal B Enzym 109:53–61, http://dx.doi.org/10.1016/j.molcatb.2014.08.007

67. Liu Q, Li H, Zhao Q, Zhu R, Yang Y, Jia Q, Bian B, Zhuo L (2014) Glucose-sensitive colorimetric sensor based on peroxidase mimics activity of porphyrin-Fe_3O_4 nanocomposites. Mater Sci Eng C 41:142–151, http://dx.doi.org/10.1016/j.msec.2014.04.038
68. Yang Z, Zhang C, Zhang J, Bai W (2014) Potentiometric glucose biosensor based on core–shell Fe_3O_4–enzyme–polypyrrole nanoparticles. Biosens Bioelectron 51:268–273, http://dx.doi.org/10.1016/j.bios.2013.07.054
69. Zhang G, Lai BB, Zhou YY, Chen BA, Wang XM, Lu Q, Chen YH (2011) Fe3O4 nanoparticles with daunorubicin induce apoptosis through caspase 8-PARP pathway and inhibit K562 leukemia cell-induced tumor growth in vivo. Nanomedicine 7(5):595–603
70. Khorramizadeh MR, Esmail-Nazari Z, Zarei-Ghaane Z, Shakibaie M, Mollazadeh-Moghaddam K, Iranshahi M, Shahverdi AR (2010) Umbelliprenin-coated Fe_3O_4 magnetite nanoparticles: antiproliferation evaluation on human fibrosarcoma cell line (HT-1080). Mat Sci Eng C-Mater 30(7):1038–1042
71. Tie SL, Lee HC, Bae YS, Kim MB, Lee K, Lee CH (2007) Monodisperse Fe_3O_4/Fe@SiO_2 core/shell nanoparticles with enhanced magnetic property. Colloid Surf A 293(1–3): 278–285
72. Larumbe S, Gomez-Polo C, Perez-Landazabal JI, Pastor JM (2012) Effect of a SiO_2 coating on the magnetic properties of Fe_3O_4 nanoparticles. J Phys-Condens Matter 24(26)
73. Abbas M, Rao BP, Islam MN, Naga SM, Takahashi M, Kim C (2014) Highly stable- silica encapsulating magnetite nanoparticles (Fe_3O_4/SiO_2) synthesized using single surfactantless-polyol process. Ceram Int 40(1):1379–1385
74. Mesarosova M, Kozics K, Babelova A, Regendova E, Pastorek M, Vnukova D, Buliakova B, Razga F, Gabelova A (2014) The role of reactive oxygen species in the genotoxicity of surface-modified magnetite nanoparticles. Toxicol Lett 226(3):303–313
75. Xia HQ, Cui B, Zhou JH, Zhang LL, Zhang J, Guo XH, Guo HL (2011) Synthesis and characterization of Fe_3O_4@C@Ag nanocomposites and their antibacterial performance. Appl Surf Sci 257(22):9397–9402
76. Arsianti M, Lim M, Lou SN, Goon IY, Marquis CP, Amal R (2011) Bi-functional gold-coated magnetite composites with improved biocompatibility. J Colloid Interface Sci 354(2): 536–545
77. Muzquiz-Ramos EM, Cortes-Hernandez DA, Escobedo-Bocardo JC, Zugasti-Cruz A (2012) In vitro bonelike apatite formation on magnetite nanoparticles after a calcium silicate treatment: Preparation, characterization and hemolysis studies. Ceram Int 38(8):6849–6856
78. Yun J-G, Lee Y-M, Lee W-J, Kim C-S, Yoon S-G (2013) Selective growth of pure magnetite thin films and/or nanowires grown in situ at a low temperature by pulsed laser deposition. J Mater Chem C 1(10):1977–1982. doi:10.1039/C2TC00672C
79. Grumezescu V, Holban AM, Iordache F, Socol G, Mogoşanu GD, Grumezescu AM, Ficai A, Vasile BŞ, Truşcă R, Chifiriuc MC, Maniu H (2014) MAPLE fabricated magnetite@eugenol and (3-hidroxybutyric acid-co-3-hidroxyvaleric acid)–polyvinyl alcohol microspheres coated surfaces with anti-microbial properties. Appl Surf Sci 306:16–22, http://dx.doi.org/10.1016/j.apsusc.2014.01.126
80. Oh CY, Oh JH, Ko T (2002) The microstructure and characteristics of magnetite thin films prepared by ultrasound-enhanced ferrite plating. IEEE T Magn 38(5):3018–3020
81. Mantovan R, Lamperti A, Georgieva M, Tallarida G, Fanciulli M (2010) CVD synthesis of polycrystalline magnetite thin films: structural, magnetic and magnetotransport properties. J Phys D Appl Phys 43(6)
82. Zhang GM, Fan CF, Pan LQ, Wang FP, Wu P, Qiu H, Gu YS, Zhang Y (2005) Magnetic and transport properties of magnetite thin films. J Magn Magn Mater 293(2):737–745
83. Qiu HM, Pan LQ, Li LW, Zhu H, Zhao XD, Xu M, Qin LQ, Xiao JQ (2007) Microstructure and magnetic properties of magnetite thin films prepared by reactive sputtering. J Appl Phys 102(11)
84. Cristescu R, Popescu C, Socol G, Iordache I, Mihailescu IN, Mihaiescu DE, Grumezescu AM, Balan A, Stamatin I, Chifiriuc C, Bleotu C, Saviuc C, Popa M, Chrisey DB (2012) Magnetic core/shell nanoparticle thin films deposited by MAPLE: investigation by chemical, morphological and in vitro biological assays. Appl Surf Sci 258(23):9250–9255

85. Andrew P (2010) Rising threat of infections unfazed by antibiotics. New York Times
86. Breathnach AS (2013) Nosocomial infections and infection control. Medicine 41(11): 649–653, http://dx.doi.org/10.1016/j.mpmed.2013.08.010
87. Grumezescu V, Holban AM, Grumezescu AM, Socol G, Ficai A, Vasile BS, Trusca R, Bleotu C, Lazar V, Chifiriuc CM, Mogosanu GD (2014) Usnic acid-loaded biocompatible magnetic PLGA-PVA microsphere thin films fabricated by MAPLE with increased resistance to staphylococcal colonization. Biofabrication 6(3)
88. Mihaiescu DE, Cristescu R, Dorcioman G, Popescu CE, Nita C, Socol G, Mihailescu IN, Grumezescu AM, Tamas D, Enculescu M, Negrea RF, Ghica C, Chifiriuc C, Bleotu C, Chrisey DB (2013) Functionalized magnetite silica thin films fabricated by MAPLE with antibiofilm properties. Biofabrication 5(1)
89. Anghel AG, Grumezescu AM, Chirea M, Grumezescu V, Socol G, Iordache F, Oprea AE, Anghel I, Holban AM (2014) MAPLE fabricated Fe_3O_4@*cinnamomum verum* antimicrobial surfaces for improved gastrostomy tubes. Molecules 19(7):8981–8994
90. Holban AM, Grumezescu V, Grumezescu AM, Vasile BS, Trusca R, Cristescu R, Socol G, Iordache F (2014) Antimicrobial nanospheres thin coatings prepared by advanced pulsed laser technique. Beilstein J Nanotechnol 5:872–880
91. Vivero-Escoto JL, Huang YT (2011) Inorganic-organic hybrid nanomaterials for therapeutic and diagnostic imaging applications. Int J Mol Sci 12(6):3888–3927
92. Simchi A, Tamjid E, Pishbin F, Boccaccini AR (2011) Recent progress in inorganic and composite coatings with bactericidal capability for orthopaedic applications. Nanomedicine 7(1):22–39
93. Guo R, Du X, Zhang R, Deng L, Dong A, Zhang J (2011) Bioadhesive film formed from a novel organic–inorganic hybrid gel for transdermal drug delivery system. Eur J Pharm Biopharm 79(3):574–583, http://dx.doi.org/10.1016/j.ejpb.2011.06.006
94. Nguyen TD (2013) Portraits of colloidal hybrid nanostructures: controlled synthesis and potential applications. Colloid Surf B 103:326–344
95. Rosu MC, Bratu I (2014) Promising psyllium-based composite containing TiO_2 nanoparticles as aspirin-carrier matrix. Prog Nat Sci-Mater 24(3):205–209
96. Yu S, Jeong SG, Chung O, Kim S (2014) Bio-based PCM/carbon nanomaterials composites with enhanced thermal conductivity. Sol Energ Mat Sol C 120:549–554
97. Yoshioka T, Chávez-Valdez A, Roether JA, Schubert DW, Boccaccini AR (2013) AC electrophoretic deposition of organic–inorganic composite coatings. J Colloid Interface Sci 392:167–171, http://dx.doi.org/10.1016/j.jcis.2012.09.087
98. Bounor-Legaré V, Cassagnau P (2014) In situ synthesis of organic–inorganic hybrids or nanocomposites from sol–gel chemistry in molten polymers. Prog Polym Sci 39(8): 1473–1497, http://dx.doi.org/10.1016/j.progpolymsci.2014.04.003
99. Wang H, Chen D, Yu L, Chang M, Ci L (2015) One-step, room temperature, colorimetric melamine sensing using an in-situ formation of silver nanoparticles through modified Tollens process. Spectrochim Acta A Mol Biomol Spectrosc 137:281–285, http://dx.doi.org/10.1016/j.saa.2014.08.041
100. Li X, Pang RZ, Li JS, Sun XY, Shen JY, Han WQ, Wang LJ (2013) In situ formation of Ag nanoparticles in PVDF ultrafiltration membrane to mitigate organic and bacterial fouling. Desalination 324:48–56
101. Katiyar V, Gerds N, Koch CB, Risbo J, Hansen HCB, Plackett D (2010) Poly L-lactide-layered double hydroxide nanocomposites via in situ polymerization of L-lactide. Polym Degrad Stabil 95(12):2563–2573
102. Fu PJ, Chen GM, Liu J, Yang JP (2009) An intercalated hybrid of polyacrylamide/layered double hydroxide prepared via in situ intercalative polymerization. Mater Lett 63(20): 1725–1728
103. Nogueira T, Botan R, Wypych F, Lona L (2011) Study of thermal and mechanical properties of PMMA/LDHs nanocomposites obtained by in situ bulk polymerization. Compos Part A-Appl S 42(8):1025–1030

104. Tran MK, Hassani LN, Calvignac B, Beuvier T, Hindre F, Boury F (2013) Lysozyme encapsulation within PLGA and $CaCO_3$ microparticles using supercritical CO_2 medium. J Supercrit Fluid 79:159–169
105. Ma F, Zhou L, Tang J, Wei SH, Zhou YH, Zhou JH, Wang FB, Shen J (2012) A facile method for hemoglobin encapsulation in silica nanoparticles and application in biosensors. Micropor Mesopor Mat 160:106–113
106. Fujiwara M, Shiokawa K, Kubota T, Morigaki K (2014) Preparation of calcium carbonate microparticles containing organic fluorescent molecules from vaterite. Adv Powder Technol 25(3):1147–1154
107. Catauro M, Papale F, Bollino F, Gallicchio M, Pacifico S (2014) Biological evaluation of zirconia/PEG hybrid materials synthesized via sol–gel technique. Mater Sci Eng C 40: 253–259, http://dx.doi.org/10.1016/j.msec.2014.04.001
108. Zu L, Li R, Jin L, Lian H, Liu Y, Cui X (2014) Preparation and characterization of polypropylene/silica composite particle with interpenetrating network via hot emulsion sol–gel approach. Prog Nat Sci 24(1):42–49, http://dx.doi.org/10.1016/j.pnsc.2014.01.001
109. Wang HA, Bongio M, Farbod K, Nijhuis AWG, van den Beucken J, Boerman OC, van Hest JCM, Li YB, Jansen JA, Leeuwenburgh SCG (2014) Development of injectable organic/inorganic colloidal composite gels made of self-assembling gelatin nanospheres and calcium phosphate nanocrystals. Acta Biomater 10(1):508–519
110. Wang XX, Song XM, Lin M, Wang HT, Zhao YL, Zhong W, Du QG (2007) Surface initiated graft polymerization from carbon-doped TiO2 nanoparticles under sunlight illumination. Polymer 48(20):5834–5838
111. Bach LG, Islam MR, Kim JT, Seo S, Lim KT (2012) Encapsulation of Fe_3O_4 magnetic nanoparticles with poly(methyl methacrylate) via surface functionalized thiol-lactam initiated radical polymerization. Appl Surf Sci 258(7):2959–2966
112. Liu P, Wang TM (2008) Poly(hydroethyl acrylate) grafted from ZnO nanoparticles via surface-initiated atom transfer radical polymerization. Curr Appl Phys 8(1):66–70
113. Zhao J, Milanova M, Warmoeskerken MMCG, Dutschk V (2012) Surface modification of TiO_2 nanoparticles with silane coupling agents. Colloid Surf A 413:273–279
114. Mallakpour S, Barati A (2011) Efficient preparation of hybrid nanocomposite coatings based on poly(vinyl alcohol) and silane coupling agent modified TiO_2 nanoparticles. Prog Org Coat 71(4):391–398
115. Sabzi M, Mirabedini SM, Zohuriaan-Mehr J, Atai M (2009) Surface modification of TiO_2 nano-particles with silane coupling agent and investigation of its effect on the properties of polyurethane composite coating. Prog Org Coat 65(2):222–228
116. Meng SW, Mansouri J, Ye Y, Chen V (2014) Effect of templating agents on the properties and membrane distillation performance of TiO_2-coated PVDF membranes. J Membrane Sci 450:48–59
117. Crippa M, Callone E, D'Arienzo M, Müller K, Polizzi S, Wahba L, Morazzoni F, Scotti R (2011) TiO_2 nanocrystals grafted on macroporous silica: a novel hybrid organic–inorganic sol–gel approach for the synthesis of highly photoactive composite material. Appl Catal B Environ 104(3–4):282–290, http://dx.doi.org/10.1016/j.apcatb.2011.03.018
118. Stathatos E, Papoulis D, Aggelopoulos CA, Panagiotaras D, Nikolopoulou A (2012) TiO_2/palygorskite composite nanocrystalline films prepared by surfactant templating route: Synergistic effect to the photocatalytic degradation of an azo-dye in water. J Hazard Mater 211:68–76
119. Birjega R, Matei A, Mitu B, Ionita MD, Filipescu M, Stokker-Cheregi F, Luculescu C, Dinescu M, Zavoianu R, Pavel OD, Corobea MC (2013) Layered double hydroxides/polymer thin films grown by matrix assisted pulsed laser evaporation. Thin Solid Films 543:63–68
120. Predoi D, Ciobanu CS, Radu M, Costache M, Dinischiotu A, Popescu C, Axente E, Mihailescu IN, Gyorgy E (2012) Hybrid dextran-iron oxide thin films deposited by laser techniques for biomedical applications. Mat Sci Eng C-Mater 32(2):296–302
121. Paun IA, Moldovan A, Luculescu CR, Dinescu M (2013) Antibacterial polymeric coatings grown by matrix assisted pulsed laser evaporation. Appl Phys A-Mater 110(4):895–902

122. Bigi A, Boanini E, Capuccini C, Fini M, Mihailescu IN, Ristoscu C, Sima F, Torricelli P (2009) Biofunctional alendronate–hydroxyapatite thin films deposited by matrix assisted pulsed laser evaporation. Biomaterials 30(31):6168–6177, http://dx.doi.org/10.1016/j.biomaterials.2009.07.066
123. Sima LE, Filimon A, Piticescu RM, Chitanu GC, Suflet DM, Miroiu M, Socol G, Mihailescu IN, Neamtu J, Negroiu G (2009) Specific biofunctional performances of the hydroxyapatite–sodium maleate copolymer hybrid coating nanostructures evaluated by in vitro studies. J Mater Sci Mater Med 20(11):2305–2316. doi:10.1007/s10856-009-3800-7
124. Ciobanu C, Iconaru S, Gyorgy E, Radu M, Costache M, Dinischiotu A, Le Coustumer P, Lafdi K, Predoi D (2012) Biomedical properties and preparation of iron oxide-dextran nanostructures by MAPLE technique. Chem Cent J 6(1):17